

Metamaterial filter for the near-visible spectrum

Haider Butt,^{1,a)} Qing Dai,¹ Niraj N. Lal,² Timothy D. Wilkinson,¹ Jeremy J. Baumberg,² and Gehan A. J. Amaratunga^{1,3}

¹Department of Engineering, University of Cambridge, Cambridge CB3 0FA, United Kingdom

²Nanophotonics Centre, Cavendish Laboratory, University of Cambridge, Cambridge CB3 0HE, United Kingdom

³Sri Lanka Institute of Nanotechnology (SLINTEC), Lot 14, Zone A, EPZ, Biyagama, Sri Lanka

(Received 3 May 2012; accepted 6 August 2012; published online 21 August 2012)

We demonstrate metamaterials operating in the near-visible regime based on two-dimensional arrays of gold-coated silicon nanopillars. The nanopillar arrays demonstrate a cutoff response at the metamaterial plasma frequency in accordance with theory and can be utilized for filtering applications. A plasma frequency in the near visible region of $\lambda = 1 \mu\text{m}$ is calculated numerically for an array with a lattice constant of 300 nm and wire radius of 50 nm, with reflection measurements in agreement with numerical calculations. Such structures can be utilized for achieving negative-index based metamaterials for the visible spectrum. © 2012 American Institute of Physics. [<http://dx.doi.org/10.1063/1.4747323>]

Metamaterials can be formed artificially by sub-wavelength components to display properties beyond those available in naturally occurring materials. Arrays of sub-wavelength structures can be engineered to exhibit the required values of permittivity and permeability in the desired frequency range. It has been reported that thin metal wire structures can be used as electrical subwavelength components for achieving artificial dielectric properties.¹ Arrays of such structures display a cutoff filtering response in the frequency domains depending on the array geometry.² These structures demonstrate plasma frequencies which can be utilized for filtering in microwave and terahertz frequency domains.³ Previously, we reported plasmonic filtering effects (in infrared wavelength range of $1.5 \mu\text{m}$) displayed by periodic arrays of multiwalled carbon nanotubes.^{4,5} The nanotube arrays were fabricated with lattice constants of 400 nm. Achieving similar metamaterial effects in the optical regime is a challenge as it requires the fabrication of uniform subwavelength wires structures with inter-spacing smaller than 400 nm.

The objective of this letter is to present such metamaterial filters which operate in the near-optical regime. Such metamaterials are realized by using two-dimensional periodic arrays of gold-coated silicon (Si) nanopillars to act as metallic nano-wire structures. Si, due to its high refractive index and low losses, is extensively used in the fabrication of photonic⁶ and electrical devices.⁷ Recent developments in nanofabrication allows us to construct nano-scaled arrays of silicon pillars or holes and utilize them as periodic refractive index media for applications like photonic crystals, solar cells, and antireflective coatings. Here, we report the unique utilization of arrays Si nanopillars for producing metamaterials operating in the near-optical regime. The highly metallic character required for achieving the metamaterial effect is achieved by coating the Si pillars with gold.⁸

Pendry *et al.*¹ demonstrated that the electromagnetic response of a metallic array composed of thin metallic wires, excited by an electric field parallel to the wires (transverse magnetic (TM) mode) is similar to that of a low-density plasma of very heavy charged particles with an effectively reduced plasma frequency ω_p providing a red-shifted plasma wavelength

$$\lambda_p = a\sqrt{2\pi \ln(a/r)}, \quad (1)$$

where a is the lattice constant of the 2D wire array, and r is the radius of the wires. The lowering of the plasma frequency is caused by the increase in the effective electronic mass within the metal wires due to the induced current and corresponding magnetic field around them. This concept can be used for achieving negative permittivity for metamaterials. According to Eq. (1), the effective plasma frequency strongly depends on the wire radius and lattice constant. Their values can independently be chosen to engineer metal wire arrays of a desired plasma frequency. The resultant frequency-dependent permittivity can be calculated using the Drude model for lossless metals described as

$$\varepsilon(\omega) = 1 - \frac{\omega_p^2}{\omega^2}. \quad (2)$$

The effective permittivity $\varepsilon(\omega)$ is negative for frequencies less than ω_p , therefore no wave propagation takes place inside the metamaterial. Electromagnetic waves propagate only at frequencies above ω_p , at which point the structure acts as a nanophotonic high-pass filter. Here, the structure is realized with square lattice array of gold-coated silicon nanopillars having radius of 50 nm and lattice constant of 300 nm. Such nanoscale metamaterial filters can be used in planar nanophotonic devices.

Theoretical calculations of the plasma frequency and reflection coefficient of such a nano-scale brush-like array were conducted. For a square lattice of nanopillars with radius 50 nm and lattice constant 300 nm, the plasma frequency

^{a)}Telephone: 44-1223-748353. Fax: 44-1223-748310. Electronic mail: hb319@cam.ac.uk.

$f_p = \omega_p/2\pi$ of 300 THz with corresponding plasma wavelength of $\lambda_p = 1 \mu\text{m}$ was calculated using Eq. (1). The value of the frequency dependent permittivity for the structure was calculated from Eq. (2). From Ref. 4, the reflection coefficient at normal incidence for such metamaterial can be calculated using Fresnel equations. While the thickness of the metamaterial was of order 1 mm for our fabricated sample, diffraction out of the nanopillar arrays restricts the propagation length to the confocal parameter of order $6 \mu\text{m}$. Therefore, the Fresnel equations were solved for a $6 \mu\text{m}$ wide array of metallic nanopillars. The calculated frequency-dependent reflection coefficient (Figure 1) shows a sharp drop in the TM reflection at the plasma frequency, with high transmission of electromagnetic waves of larger frequencies. The small peaks in the plot arise from multiple reflections at the metamaterial interfaces. The metamaterial filtering effect is produced primarily due to the metallic nature (gold coating) of the nanopillars. Such effects are not observed in conventional Si nanopillar arrays with similar dimensions. Periodic arrays of Si nanopillars/holes rather act as photonic crystals which display photonic band gaps (due to Bragg diffraction) in the wavelength regimes near $(\lambda \approx 2a)$.⁹

To achieve this metamaterial high pass filter in the optical domain, metallic cylinders of nano-scale dimensions and interspacing are required. Si nanopillars are promising materials to establish such metamaterials structures with advancement in nanotechnology facilitating the fabrication of high a/r aspect ratio nanopillars arrays with a high order of periodicity. The growth of such high a/r aspect ratio arrays of silicon nanopillars is significantly difficult and achieved only through careful optimization of growth parameters. The fabrication was performed using e-beam lithography to make the dot array pattern ($r = 50 \text{ nm}$, $a = 300$) on the Si substrate. The pattern was then sputtered with a 200 nm thick metal mask (tungsten). The process of deep reactive etching (DRIE) was performed for etching the substrate. The array was then exposed to the following gases for a second each, in a succession lasting for 5 min: C_4F_8 for protective layering, SF_6 for etching, and O_2 for removing the SF_6 residues. The final etched substrate was over-coated with approxi-

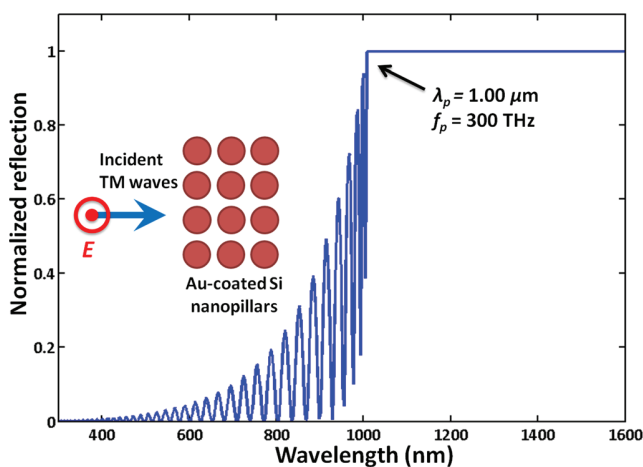


FIG. 1. The calculated TM mode reflection spectra for gold-coated silicon nanopillars based high pass filter. In TM mode, the incident light is polarized parallel to the wire structures and at the plasma frequency f_p of 300 THz ($\lambda_p = 1.00 \mu\text{m}$) a sharp drop in reflectivity is calculated.

mately 10 nm of gold using thermal evaporation. Scanning electron micrographs (Figure 2) show well aligned and periodically patterned Si nanopillars. At some regions, the pillars were tapered due to non-uniform deposition of the metal mask. Deposits of tungsten mask layer are also observed on the tips of nanopillars, which cause slight scattering loss. Both these issues can be improved by optimizing the metal mask layer deposition and thickness.

Si nanopillars with an average height of $1 \mu\text{m}$ were produced by the etching process. The metal mask on the nanopillar tips was over-coated by the evaporated gold layer which increased the effective height of nanopillars to about $1.25 \mu\text{m}$. Longer Si pillars can be achieved by using thicker Si substrates. A steady periodicity required for a 2D square lattice array based metamaterial was common throughout the sample. According to metamaterial theory, it is crucial that the wire structures are thin compared to the operating wavelengths. Without the effect of thin wires, the plasma wavelength λ_p is of the same order as the lattice constant producing diffraction effects. Using thin wires increases the plasma wavelength and reduces the diffraction effects. Therefore, a nanopillar array with spacing of 300 nm and radius of 50 nm was adequate for studying the metamaterial with a plasma wavelength of $\lambda_p = 1 \mu\text{m}$.

The sample was characterized using a goniometer setup to obtain reflection spectra. A supercontinuum white-light laser (Fianium) was utilized for illumination with wavelength range 380 nm to 1600 nm. The polarization of the

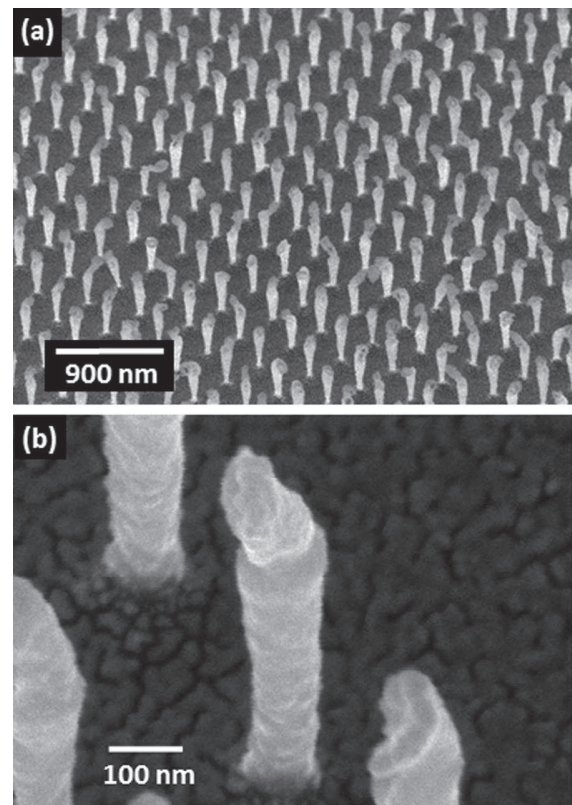


FIG. 2. (a) Electron microscopy image of a 2D square lattice array of gold coated Si nanopillars with radius of 50 nm and lattice constant of 300 nm. (b) The same in higher resolution. The tungsten mask can be observed on the nanopillars tip.

white-light laser beam was selected before the beam was guided onto the sample. Reflectance is confocally collected and fiber-coupled via a beam splitter to two Ocean Optics spectrometers (QE65000 and NIRQuest) allowing measurement of the broad spectral range of 380–1600 nm.

Measured reflection spectra for light polarized parallel (TM) and perpendicular (TE) to the nanopillars are shown in Figure 3. The measurements were taken at incident angles ranging from 60° to 70° with a resolution of 1°. Figures 3(a) and 3(b) show individual spectra at angles of 60°, 65°, and 70°. A rapid change in reflection is observed for the TM mode (light polarized parallel to nanopillars) at 1 μm which closely matches the calculated plasma wavelength of the metamaterial. After approximately 1 μm , the sample displays a high-reflectivity towards all the wavelengths bigger than the plasma wavelength λ_p , acting as a high pass filter. Additional reflection peaks are observed at 600 nm and smaller wavelengths, explained by the diffraction effects which are dominant at this wavelength regime ($\lambda/2 \approx a$). Reflectance for light polarized perpendicular (TE) to the nanopillars does not show any significant cut-off effect near the 1 μm part of the spectrum, in accordance with theory. TE light produces transverse electronic motion on the nanopillars, but due to their small radius compared

to the array lattice constant no significant mutual coupling effects take place. Hence, no TE related cut-off response is observed. There is a strong dip observed in the TE spectrum at 600 nm corresponding to the diffraction of light satisfying the Bragg condition $\lambda/2 \approx a$, where $a = 300$ nm for the nanopillars array.

The angular dependence of both the metamaterial filtering effect (in TM mode) and diffraction (in TE mode) can be observed in Figures 3(a) and 3(b). With varying incident angles, the effective lattice constant and pillar length observed by the incident light varies, causing slight shifts in the measured spectra. However, the metamaterial cut-off filtering effect (near the wavelength of 1 μm) is the dominating and persistent effect observed for all the TM mode spectra, while only diffraction related dips are observed in the TE mode spectra below the 600 nm wavelength. Mie theory calculations predict that some scattering and absorption effects are also expected below the wavelengths of 500 nm from the tungsten deposits present on the tips of nanopillars. However, such effects are minimal around the wavelength of interest 1 μm .

A rapid drop in reflection at λ_p for parallel polarized light shows the periodic array of gold coated Si pillars acts as a high-pass filter for near-visible frequencies. The plasma frequency for the metamaterial can be further tuned into the optical regime by increasing the material density of the sample, i.e., by increasing the radius of the pillar and decreasing the lattice constant as presented in Eq. (1) This would also push diffraction effects towards shorter wavelengths, enhancing the high-pass filter effect. The arrays of gold coated Si nanopillars can also be used for achieving negative index materials which operate in the optical regime. Our studies show that metallic nanopillars arrays display negative permittivity. By integrating these nanopillars arrays with magnetic subwavelength structures (such as nano-split ring resonators), both negative permittivity and permeability can be achieved simultaneously.¹⁰ Such materials could display negative index and achieve applications such as cloaking and super-lensing in the visible spectrum.

In conclusion, we demonstrate a near-visible high pass filter based on a 2D square lattice array of gold-coated Si nanopillars. Arrays of metallic nanopillars having lattice constants of 300 nm and radius of 50 nm act as metamaterials displaying a plasma cut-off frequency of approximately 300 THz (1 μm). A rapid drop in reflection spectrum was calculated at the plasma frequency. The polarization-sensitive measured filtering response is in agreement with the theory of these materials. The study shows that by using gold-coated Si nanopillars, metamaterials effects can be achieved in the optical regime. Future applications include the designing of negative index materials operating in the visible spectrum.

This work was supported by EPSRC EP/G060649/1. This work was also partly funded under the Nokia-Cambridge Strategic Partnership in Nanoscience and Nanotechnology (Energy Programme).

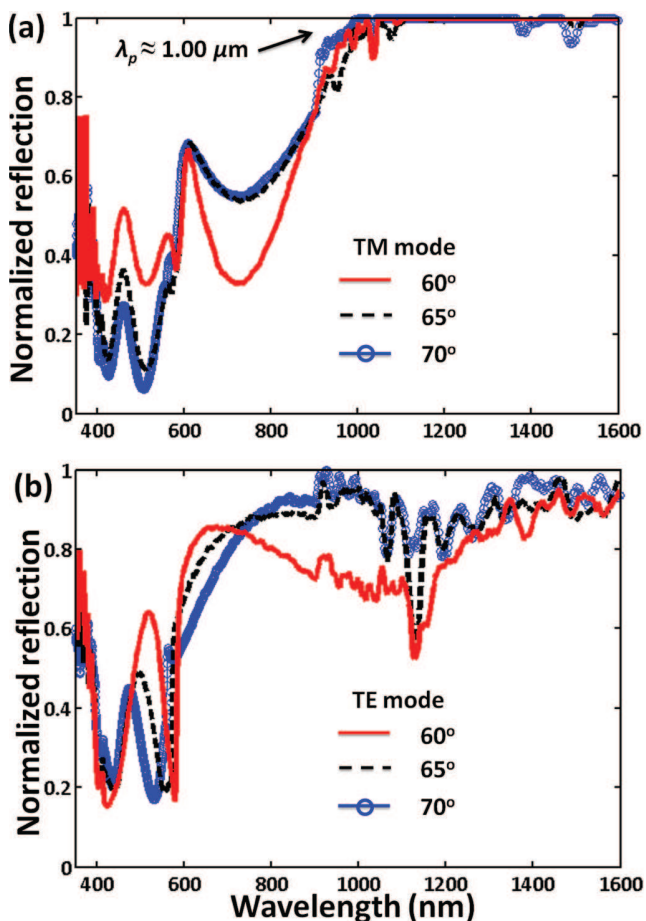


FIG. 3. The reflection spectra measured at individual angles for light polarized (a) parallel (TM mode) and (b) perpendicular (TE mode) to the gold coated Si nanopillars. A sharp drop in the reflected TM mode is observed at plasma frequency ($\lambda_p = 1.00 \mu\text{m}$), matching closely with theory.

¹J. B. Pendry, A. J. Holden, W. J. Stewart, and I. Youngs, *Phys. Rev. Lett.* **76**, 4773 (1996).

²D. Wu, N. Fang, C. Sun, X. Zhang, W. J. Padilla, D. N. Basov, D. R. Smith, and S. Schultz, *Appl. Phys. Lett.* **83**, 201–203 (2003).

- ³P. Gay-Balmaz, C. Maccio, and O. J. F. Martin, *Appl. Phys. Lett.* **81**, 2896–2898 (2002).
- ⁴H. Butt, Q. Dai, P. Farah, T. Butler, T. D. Wilkinson, J. J. Baumberg, and G. A. J. Amaratunga, *Appl. Phys. Lett.* **97**, 163102 (2010).
- ⁵H. Butt, Q. Dai, R. Rajasekharan, T. D. Wilkinson, and G. A. J. Amaratunga, *ACS Nano* **5**, 9138–9143 (2011).
- ⁶H. Butt, Q. Dai, R. Rajasekharan, T. D. Wilkinson, and G. A. J. Amaratunga, *Appl. Phys. Lett.* **99**, 133105 (2011).
- ⁷H. Zhou, A. Colli, A. Ahnood, Y. Yang, N. Rupesinghe, T. Butler, I. Haneef, P. Hiralal, A. Nathan, and G. A. J. Amaratunga, *Adv. Mater.* **21**, 3919–3923 (2009).
- ⁸Y.-S. Chen, W. Frey, S. Kim, P. Kruiyinga, K. Homan, and S. Emelianov, *Nano Lett.* **11**, 348–354 (2011).
- ⁹T. Xu, N. Zhu, M. Y. C. Xu, L. Wosinski, J. S. Aitchison, and H. E. Ruda, *Appl. Phys. Lett.* **94**, 241110 (2009).
- ¹⁰D. R. Smith, J. B. Pendry, and M. C. K. Wiltshire, *Science* **305**, 788–792 (2004).